Scripta Materialia 133 (2017) 24–28

Contents lists available at ScienceDirect

Scripta Materialia

journal homepage: www.elsevier.com/locate/scriptamat

Regular article

Revealing the shear band cracking mechanism in metallic glass by X-ray tomography

R.T. Qu *, S.G. Wang, X.D. Wang, Z.Q. Liu, Z.F. Zhang *

Shenyang National Laboratory for Materials Science, Institute of Metal Research, Chinese Academy of Sciences, 72 Wenhua Road, Shenyang 110016, China

ARTICLE INFO

Article history:
Received 21 December 2016
Received in revised form 2 February 2017
Accepted 10 February 2017
Available online xxxx

Keywords:
Metallic glass
Shear band
Cracking
X-ray tomography
Compression

ABSTRACT

The mechanism of shear band (SB) cracking or cavitating under the stress state free from negative pressure is one of long-standing unsolved issues in metallic glass (MG). Here we show key findings including the 3D imaging on the evolution of SB cracking during compressing a ductile MG. Discontinuous and non-coplanar cracks with long-narrow-thin morphology were observed in a shear-banding affected zone that is much thicker than the SB core. The results demonstrated that the SB cracking originates possibly from (1) the creation and coalescence of excess free volume, (2) the shearing of non-planar SB, and/or (3) the SB interaction.

Usually, shear band (SB) acts as the main plastic deformation carrier and the origin of failure in metallic glasses (MGs) [1]. Knowing how SB initiates, propagates and fails, therefore, becomes the key to understand the unique mechanical behaviors of MGs [2,3] and to achieve better properties by controlling shear-banding [4]. While great strides have been made in understanding the initiation and propagation of SB, only limited attention has been concentrated on how SB fails. Since the characteristic dimension of SB, i.e., nanometer-scale thickness but millimeter-scale length, it is quite challenging to experimentally study the origin of SB failure. By far, the experimental efforts on the failure of SB mainly employ postmortem methods including: (1) deducing fracture mechanism based on fracture surface morphology [5–11]; (2) observing SB cracking on the sample surface and polished sections [12–14]. While much knowledge has been gained, due to the limitations of postmortem tests, how SB evolves into crack under loading mode without negative pressure (such as compression) is still one of key unsolved puzzles for MGs [4].

Since the non-destructive, high penetrability, and high spatial resolution attributes, the 3D X-ray tomography (XRT) has been widely applied to study the fracture mechanisms of materials [15,16]. With the development of X-ray source, detectors and the optical devices, the current lab-based 3D XRT system can achieve a high spatial resolution of 1 μm or even down to dozens of nanometers. Although this may also be larger than the thickness of SB (~10 nm [17]), it is much smaller than the width of the softening region around the SB core (e.g., 40–160 μm [18]). In this work, we studied the evolution of SB cracking in a MG by using 3D XRT combined with 2D scanning electron microscope (SEM). The 3D XRT imaging on the internal shear-banding cracks and their evolution, for the first time to our knowledge, was successfully obtained.

A ductile MG with the composition of $Zr_{65}Fe_5Al_{10}Cu_{20}$ (at.%) was selected [19]. The compressive samples with dimensions of $\sim 2 \times 2 \times 4$ mm^3 were cut from the as-cast amorphous plate and subsequently ground and polished. The compression tests were performed at a strain rate of $\sim 10^{-4}$ s^{-1} using an Instron 5982 testing machine equipped with a linear variable differential transformer (LVDT) for measuring the sample displacement. The deformation and cracking features were observed with a Leo Supra 35 SEM. The internal cavitations in deformed samples were examined using the 3D high-resolution transmission XRT technique with the lab-based Xradia Versa XRM-500 system. The working accelerating voltage was 140 kV. A total of 1600 2D projections, each of which was exposed for 5–10 s, were recorded as the sample was rotated by 360° and computationally reconstructed via a filtered back projection algorithm to visualize the internal cracks inside the sample in 3D space. The evolution of SB cracking was studied in a quasi-in situ manner. After compression to a certain plastic strain, the sample was unloaded and examined by SEM and XRT to detect the external and internal damage features. Three cycles of compression and imaging were conducted. For the XRT observation, depending on the sampling volume, the pixel size is as small as 2.31 μm, which will be specifically indicated in the captions of XRT images.

Fig. 1(a) shows the engineering stress-strain curve of the MG in the first-time compression with the corresponding deformation features exhibited in Fig. 1(b)–(f). A large shear offset of ~288 μm, which corresponds to a global plasticity of ~5.4% [20], was produced due to the

---

* Corresponding authors.
E-mail addresses: rtqu@imr.ac.cn (R.T. Qu), zhfzhang@imr.ac.cn (Z.F. Zhang).

http://dx.doi.org/10.1016/j.scriptamat.2017.02.018
1359-6462/

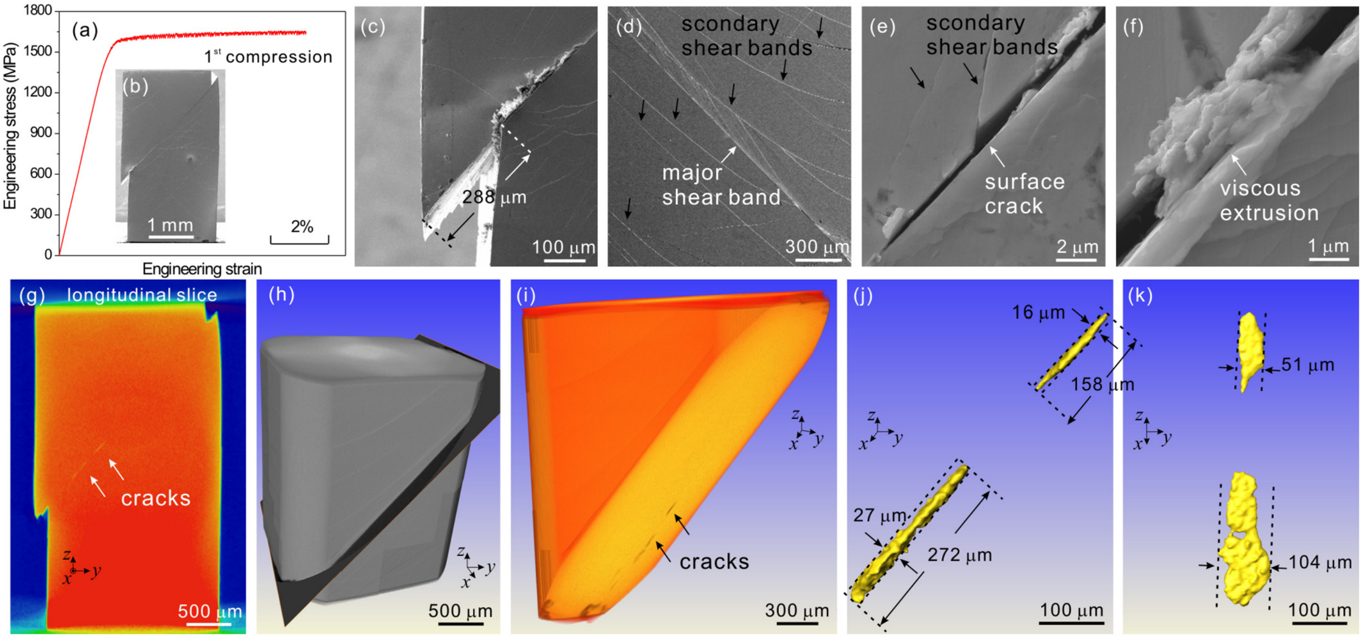

Fig. 1. SB cracking behavior after the first-time compression. (a) Engineering stress-strain curve; (b)–(f) SEM observations on the deformation and damaging features; (g)–(k) XRT observations and characterizations on the internal cracks. (j)–(k) also show the sizes of 3D cracks in the shear direction (crack length), in the direction perpendicular to shear direction in the shear band plane (crack width) and in the direction normal to the shear band plane (crack thickness). The pixel size for XRT imaging of (g) is 6.13 μm, while for others it is 2.31 μm.

sliding propagation of the major SB (MSB). The smaller value of plasticity contributed by the MSB than that measured from the stress-strain curve indicates the considerable deformation in other SBs (see Fig. 1(d)). Surface cracks and viscous extrusions can be frequently seen inside the MSB (e.g., Fig. 1(e)–(f)), conforming to the previous findings [10,14,21]. Note that at the intersection point of a secondary SB (SSB) and the MSB (Fig. 1(e)), a shear step was observed, resulting in the local expansion of surface crack.

The XRT images of the deformed sample are presented in Fig. 1(g)–(k). At a longitudinal XRT slice (Fig. 1(g)), some features like internal cracks can be readily observed. To confirm this, finer XRT imaging was conducted by focusing on the deformation part of the sample (Fig. 1(h)) to improve the spatial resolution. Fig. 1(i) presents the XRT image of the SB plane (the black plane in Fig. 1(h)), which vividly includes the appearance of internal cracks, demonstrating the occurrence of SB cracking. The 3D XRT images of the cracks can be further extracted and shown in Fig. 1(j)–(k). Two individual cracks with different dimensions can be seen, implying a discontinuous crack initiation and evolution process. Surprisingly, the thickness of the cracks is 16–27 μm, considerably larger than the thickness of embryonic SB (~10 nm). Besides, considering the long and narrow shape of the cracks, a mechanism of shear-induced crack extension should be included for the propagation of SB cracking.

In the second-time compression, further plastic strain of ~3.7% was introduced in the same MG sample, as shown in Fig. 2(a). The shear offset of the MSB increased by ~185 μm (see Fig. 2(b)), contributing to a global plastic strain of ~3.5%, which indicates that the plastic deformation was mainly carried out by the MSB. Fig. 2(c)–(e) present the XRT

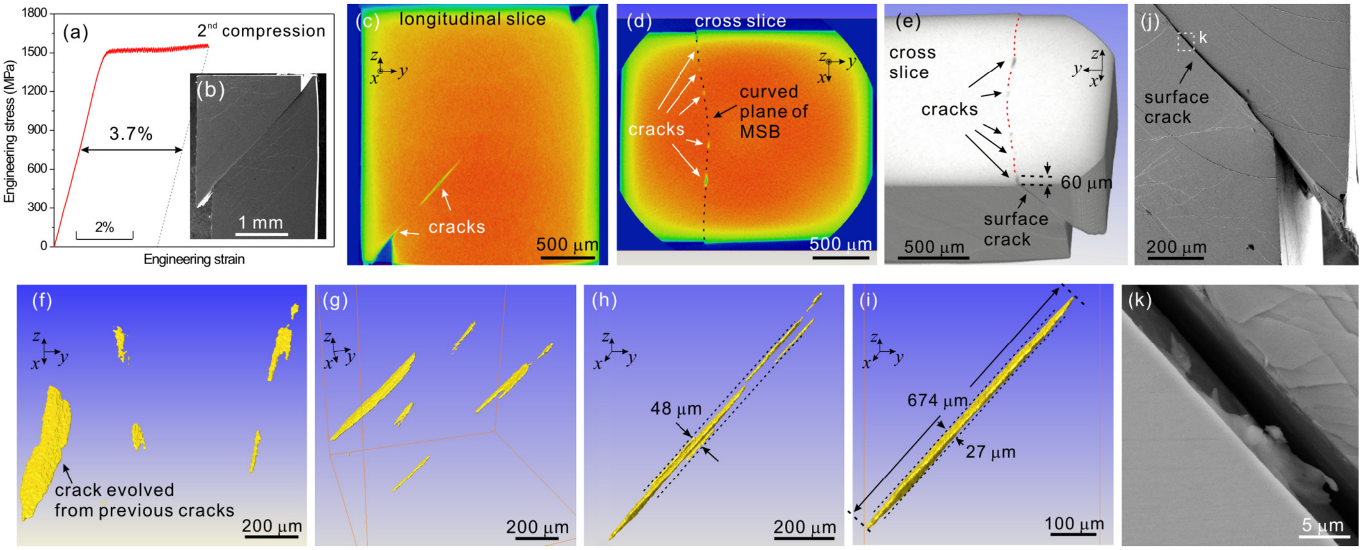

Fig. 2. SB cracking behavior after the second-time compression. (a) Engineering stress-strain curve during the second loading; (b) and (j)–(k) SEM observations on the deformation features; (c)–(i) XRT observations and characterizations on the internal cracks. The pixel size for XRT imaging is 2.48 μm.